

A STUDY OF THE PHYSICAL PROPERTIES AND STRUCTURAL DEVELOPMENT OF CLAYS IN THE SHALLOW METHANE HYDRATE FIELDS

* Koichi Nakamura¹

¹ Faculty of Engineering, Tottori University, Japan

*Corresponding Author, Received: 16 May 2023, Revised: 21 July 2023, Accepted: 2 Aug. 2023

ABSTRACT: The physical and consolidation properties of sediments were investigated using borehole cores collected from the Sakata Knoll, where shallow methane hydrate fields exist, and from nearby sites where methane hydrate is not present. The soil particle density, grain size distribution, liquid limit, plastic limit, and plasticity index were similar at all depths. The void ratio change with depth was approximately $e=3$ near the seafloor, decreased to approximately $e=2$ at approximately 20 meters below the seafloor, and remained almost unchanged until approximately 56 meters below the seafloor. This void ratio change was found to be similar to that of the seafloor in the Joetsu Basin, which has shallow methane hydrate fields. The degree of soil structure development was examined by performing incremental loading consolidation tests on the collected core samples. Structural coefficient A values indicated that structure developed with increasing depth in both cores, but the degree of structural development was small regardless of whether the cores were in the Methane hydrate bearing area or not.

Keywords: Marine clay, Consolidation, Compression, Structure

1. INTRODUCTION

Methane hydrate (MH) is a caged crystalline structure in which water molecules are incorporated by polyhedral methane molecules [1]. MH is distributed on seafloors, lake bottoms, and permafrost zones where stable low-temperature and high-pressure conditions are met. MH distributed in the seas around Japan can be roughly classified into two types: sandy-layer type (sandy-layer pore-filling type) and surface-layer type. The MH in the Japan Sea is of the shallow type and occurs in clumps or layers of mud layers [2-5]. Three areas have been identified as model study areas for surface-type MH in the Sea of Japan: off Sakata (Mogami Trough), off Joetsu (Umitaka Spur and Joetsu Basin), and north of the Tango Peninsula (Oki Trough) (Fig.1) [6].

It has been determined that existing technologies for subsea oil and natural gas development can be applied to the recovery of sand-type MH. Two offshore production tests have already been conducted, and an onshore production test is underway for a long-term production [7]. In this production method, MH is decomposed and recovered in the form of a gas by drilling a well and pumping water up to the reduced pressure in the formation. Because of this production method, studies on the strength properties of sediments have been conducted using experimental equipment that can reproduce the temperature and stress conditions of the deep sea floor, and studies on the deformation

characteristics of MH in the sand layer and after MH recovery has been conducted [8,9]. In contrast, shallow-type MH is different from sand-type MH in terms of the type of MH present, so a new recovery technique was studied. As a result, a wide-area vertical mining method using a large-diameter drill was identified as a promising technology and will be studied in the future [10]. This method involves direct drilling of MH and the ground to recover MH.

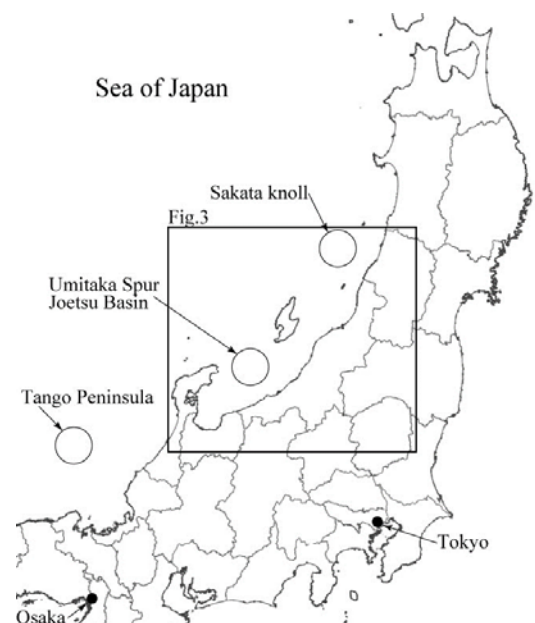


Fig.1 Study areas for surface-type MH in the Sea of Japan

Since the recovery of MH targets surface-type methane hydrate with a methane hydrate stable basement depth (BGHS) of approximately 100 m below the seafloor surface, it is necessary to drill through soil layers that are not MH-forming layers, and it is important to understand the deformation characteristics of the ground.

The sedimentation rate in the offshore areas of Sakata and Joetsu, which are the subject of this study, is estimated to be approximately 25-50 cm/ky [11,12], which means that it takes approximately 200,000-400,000 years to deposit 10 m of sediment. Therefore, the soil structure may have been influenced by age effects such as cementation and secondary consolidation [13]. For this reason, naturally deposited clays with well-developed structures are difficult to represent by simple models such as the conventional calculation method. Clay soils can be described as highly structured if the void ratio is large and as poorly structured if the void ratio is small for the same consolidation pressure.

Studies conducted on soil structure using e -log p curves obtained from one-dimensional consolidation tests can be found in Burland [14] and Tsuchida [15]. In this study, we investigate the degree of structural development in the shallow methane hydrate fields of the Sakata Knoll using the method proposed by Udaka et al. [16] to evaluate the structure of natural marine clay soils using the ultimate standard compression curve (USC) proposed by Tsuchida. Fig.2 shows a schematic representation of the compression curve in terms of the relationship between consolidation pressure p , specific volume v ($v=1+e$), and the structural coefficient A , which indicates the degree of structural development. USC is the $\ln v$ and $\ln p$ relationship when the clay is consolidated from a high water content (e.g., more than four times the liquid limit) and the consolidation pressure is sufficiently large. The structure Factor A is the

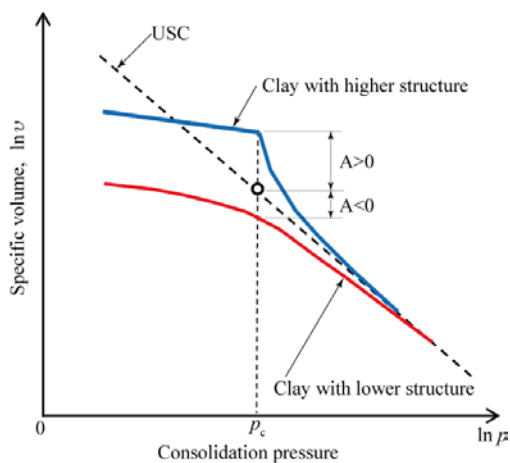


Fig.2 Compression curve model of clay using USC and structural coefficient

longitudinal distance from the USC at $p = p_c$, where a larger A indicates a highly porous structure and a smaller A , especially if it is negative, indicates a low structure.

There are a few examples of studies of the physical properties and pore ratio changes of the Japan Sea floor at a sufficient distance from land in the depth direction. Therefore, there is a lack of basic data on the physical and mechanical properties of the Japan Sea floor, which is necessary for the study of surface-type MH recovery methods. When studying the consolidation characteristics, it is necessary to consider the degree of structural development. However, the only previous studies on structural development using undisturbed marine clay samples are those on the seabed of Osaka Bay [15,19]. Furthermore, there are no examples of studies of the degree of structural development using samples collected from sites with different MH availability.

This study used core samples collected from the seafloor in the MH-bearing zone off the coast of Sakata, Yamagata Prefecture, Japan. The study consisted of the variation of physical properties and natural void ratio with depth and the degree of structural development using the results of incremental consolidation tests. The physical properties and natural void ratio were investigated using the results of the off-Joetsu seafloor [17], which had been previously investigated, and data from the literature [18], which investigated the physical properties of the seafloor at Umitaka Spur and Joetsu Knoll. Using these results, we investigated the characteristics of the void ratio change with depth and the influence of the presence of MH on the degree of structural development.

2. RESEARCH SIGNIFICANCE

In FY2021, we conducted a study using core samples up to about 55 mbsf collected from the seafloor in the MH germplasm area off the coast of Sakata, Yamagata Prefecture. The results show the characteristics of pore ratio change with depth and the influence of MH presence on the degree of structural development. The results of this study can be used as basic data of seafloor ground for the study of surface type MH recovery methods.

3. SURVEY AREA AND SAMPLING METHOD

The core samples used were collected from the Sakata Knoll (Mogami Trough) in the "Ground Strength Survey in shallow methane hydrate fields off Sakata" conducted in 2021 by the National Institute of Advanced Industrial Science and Technology (AIST). The research area was approximately 50 km offshore of Sakata City,

Yamagata Prefecture. The core samples were collected by rotary boring, and the water depth near the sampling point was approximately 550 m. The core samples were collected from RC2101A and RC2102A, and the area with the fewest cracks was selected for the experiment based on the results of X-ray CT scans. The sampling points of the specimens used in this study are shown in Fig.3, and the depths and core IDs are listed in Table 1. The cores were transported in a vacuum and with refrigerated storage on board a ship. The sampling site was located on the southwestern margin of the Akita Basin, which is an anticlinal structure formed by the tectonic inversion of the eastern margin of the Japan Sea, and muddy sediments cover the seafloor [20]. LWDs (simultaneous drilling logging) have confirmed the presence of surface-type MH [21]. The offshore Sakata area is an MH germplasm area, but detailed exploration has confirmed the presence of MH in the vicinity of RC2102A, while RC2101A is a site where MH is not confirmed. RC2101A and RC2102A are approximately 1.5 km apart.

Fig.3 and Table 1 also show the reference sampling sites used in this study, and the core names are the same as in the previous reference [17, 18]. These sites are shallow methane hydrate fields and were surveyed by the AIST. Hereafter, samples collected off the Sakata seafloor are referred to as SAKATA, and those from the Umitaka Spur, Joetsu Basins, and the Joetsu Knoll are referred to as JOETSU.

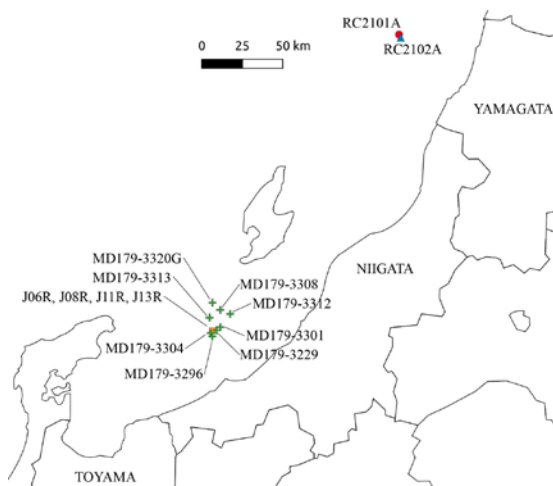


Fig.3 Location of the Sakata Knoll and Joetsu Basin

Table 1 Core name and Sampling sites

Core Name	Sampling sites
RC2101A, RC2102A	Sakata Knoll (Mogami Trough)
J06R, J08R, J11R, J13R	Umitaka Spur
MD179-3296-MD179-3320	Umitaka Spur Joetsu Basin

MD179-3296-MD179-3320 are taken from the references for soil particle density, water content, and void ratio. Although the borehole locations of J06R, J08R, J11R, and J13R were different, they are shown together in Fig.3 because the locations are close.

4. EXPERIMENTAL METHOD

4.1 Physical Properties

For the soil particle density test, a portion of the consolidation specimen was used, and for the liquid limit test and plastic limit test, combined specimens from the post-consolidation test and the portion remaining from the consolidation specimen were used. Wet density and void ratio were obtained from the soil specimens for the incremental loading consolidation tests. Particle size distribution was measured using a laser diffraction particle size analyzer (Shimadzu SALD-3100). Samples were dispersed in 0.2% sodium pyrophosphate solution ($\text{Na}_4\text{P}_2\text{O}_7 \cdot 10\text{H}_2\text{O}$) using an ultrasonication device and a magnetic stirrer.

4.2 Mineral Composition

The mineral composition of the core samples was determined by powder X-ray diffraction (XRD) with the preferred orientation method.

In the preferred orientation method, ethylene glycol-treated samples were also measured to determine the presence or absence of smectite, which has a significant impact on the decomposition conditions of methane hydrate and the activity level of sediments. This is a method to discriminate between chlorite and smectite, which have overlapping peaks in the diffraction pattern. The peaks of both minerals are separated using the swelling effect of smectite (expansion of the interlayer distance of sheet-like crystals). Specifically, a desiccator containing ethylene glycol was prepared in a thermostatic bath at 50 °C, and a sample spread on a glass slide was placed in the desiccator filled with ethylene glycol vapor for 1 hour. After this treatment, XRD analysis was performed immediately. The X-ray diffractometer used was a Rigaku RINT2500V. The measurement conditions were as follows: X-ray: CuK α , tube voltage and current: 40 kV and 160 mA, respectively. The scan range was 3 to 70°, the sampling width was 0.02°, and the scan speed was 12.0°/min. However, to examine the main peak of calcite in detail, the scan range of 28.5 to 30.5° was separately measured with a sampling width of 0.004° and a scan speed of 0.5°/min. For the stereotaxic analysis of clay, the scan range was 2 to 40°, sampling width was 0.02°, and scan speed was 8.0°/min.

5. PHYSICAL PROPERTIES

5.1 Cores

Fig.4 shows a photograph of the specimen used for the consolidation tests. The specimens were taken from the depths shown in Table 2, with the upper part on the right side of the photo and a core diameter of 75 mm. The specimens for the incremental loading consolidation tests were prepared from these specimens. The color was grayish brown regardless of the sampling depth.

Table 2 Physical properties

(a) RC2101A					
Core ID	depth (mbsf)	ρ_s (Mg/m ³)	w (%)	e	w/w _L
Core 2	1.02 - 2.00	2.664	108.3	2.886	1.049
Core 4	2.96 - 3.83	2.578	91.1	2.348	0.983
Core 12	10.41 - 11.37	2.662	87.4	2.326	0.854
Core 20	18.12 - 19.04	2.685	71.1	1.909	0.786
Core 29	26.75 - 27.70	2.635	78.1	2.059	0.814
Core 37	34.17 - 34.59	2.677	70.6	1.889	0.702
(b) RC2102A					
Core ID	depth (mbsf)	ρ_s (Mg/m ³)	w (%)	e	w/w _L
Core 1	0.00 - 0.98	2.696	105.5	2.843	1.097
Core 13	25.37 - 25.88	2.576	65.1	1.678	0.656
Core 22	54.30 - 55.12	2.574	81.4	2.094	0.821



Fig.4 Core Samples

5.2 Soil Particle Density and Particle Size Distribution

Table 2 shows the soil particle density (ρ_s), water content (w), and void ratio (e). Fig.5 shows the relationship between depth and soil particle density. The values for JOETSU and SAKATA were 2.5 to 2.8 Mg/m³ and approximately 2.6 Mg/m³, respectively, regardless of depth. Fig.6 shows the grain size accumulation curves for each core. Fig.6 shows that the grain size distribution is almost the same regardless of the sampling depth. It was also found that the grain size distribution was almost the same as that of the JOETSU samples [17].

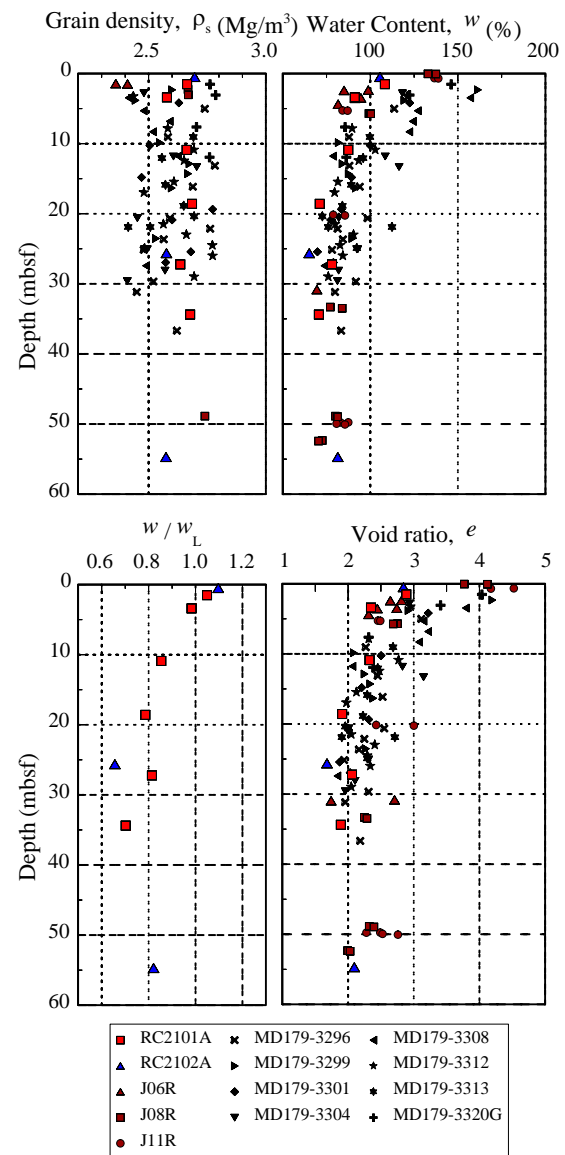


Fig.5 Vertical distribution of measured physical properties of clay in the Sakata Knoll and Joetsu Basin

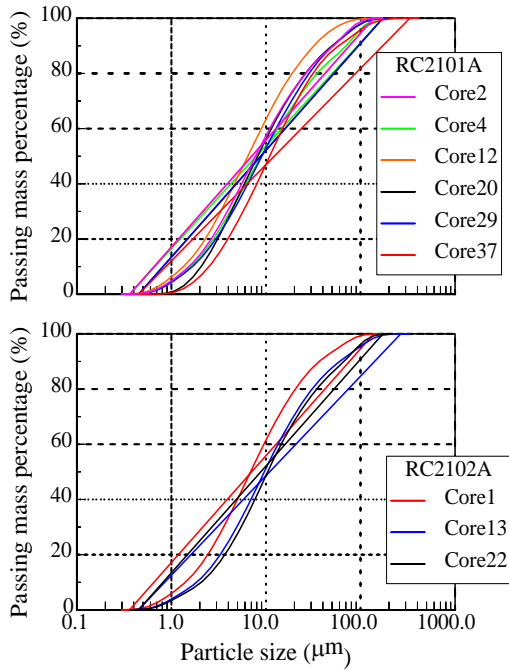


Fig.6 Grain size distribution curve of Sakata Knoll

5.3 Plasticity Index and Mineral Plasticity

Table 3 shows the liquid limit, plastic limit, plasticity index, and activity. The J13R results are also shown in the plasticity diagram in Fig.7. The plasticity diagram shows that both the SAKATA and JOETSU samples plot near the A-line around w_L 100%. In the SAKATA samples, only core 29 is classified as CH, while the others are classified as MH. Fig.8 shows w_L and w_P in the vertical direction. It is found that w_L is approximately 100% and w_P is approximately 40% regardless of depth in SAKATA.

The activity is considered to be greater than 1.25 [22]. Table 3 shows that the activity of all samples is high. Therefore, XRD analysis was conducted. Fig.9 shows the XRD results of the untreated and ethylene glycol-treated samples. The low angle range of 10° or less, where the difference between the samples with and without ethylene glycol treatment is observed, is enlarged. In Fig.9, chlorite and smectite are shown as ChlSm before ethylene glycol treatment, chlorite as Chl(EG), and smectite as Sm(EG) after ethylene glycol treatment. The peaks of smectite and chlorite were separated by ethylene glycol treatment even when the sampling depth increased, and it was confirmed that smectite and chlorite were contained in all core samples measured. This suggests that the reason for the high activity is due to the presence of smectite.

The results of 4.2 and 4.3 indicate that the physical properties of the seafloor off Sakata are almost the same up to approximately 56 mbsf.

Table 3 Plasticity index and Activity

(a) RC2101A

Core ID	w_L (%)	w_P (%)	I_p	Activity
Core 2	103.2	38.8	64.4	4.2
Core 4	92.7	39.6	53.1	3.3
Core 12	102.4	36.5	65.9	3.6
Core 20	90.5	37.0	53.5	5.1
Core 29	96.0	44.5	51.5	3.8
Core 37	100.5	40.0	60.5	8.4

(b) RC2102A

Core ID	w_L (%)	w_P (%)	I_p	Activity
Core 1	96.2	35.5	60.7	3.6
Core 13	99.3	35.8	63.5	5.4
Core 22	99.2	44.5	54.7	5.4

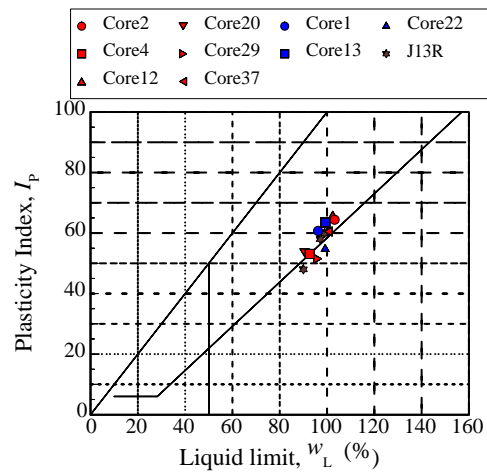


Fig.7 $I_p - w_L$ relationship of Sakata Knoll

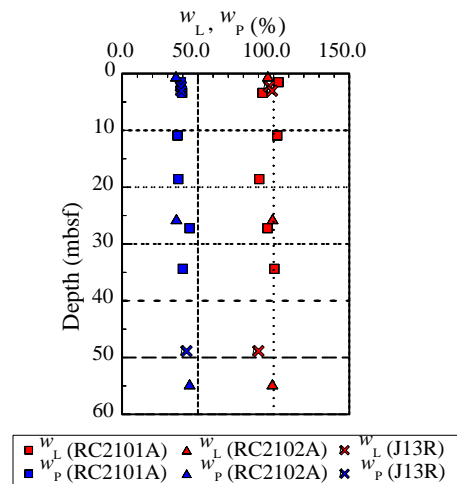


Fig.8 Vertical distribution of measured w_L and w_P of Sakata Knoll

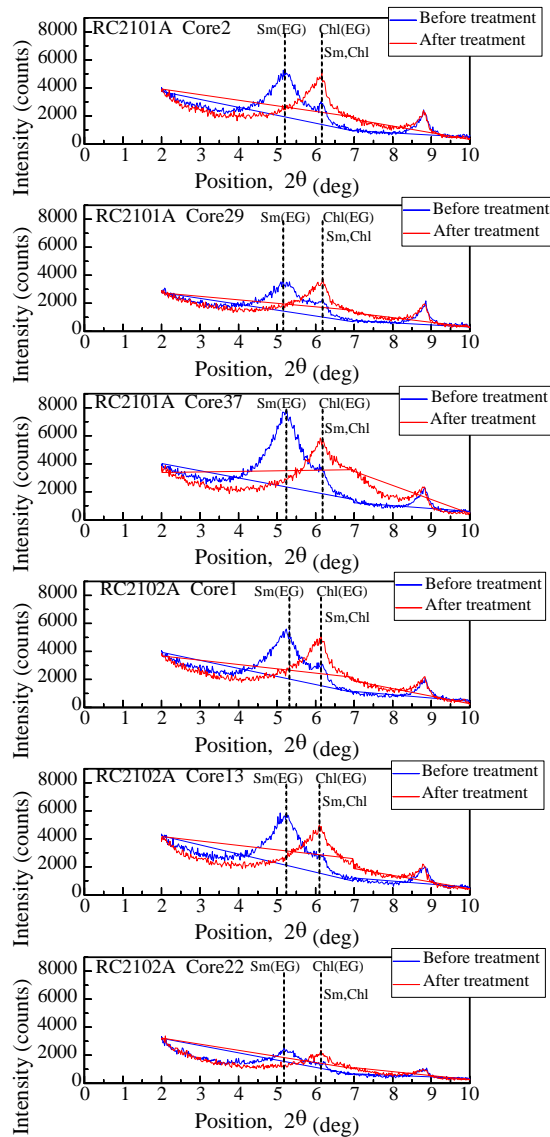


Fig.9 XRD patterns of clay minerals from Sakata Knoll

5.4 Water Content by Depth, Void Ratio, and Normalized Water Content

The water content in SAKATA decreased from approximately 105% near the seafloor surface to approximately 90% at approximately 4 mbsf with increasing depth, and the change in water content at depths below the seafloor was small. The water content at JOETSU decreased from approximately 150% near the seafloor to approximately 90% at approximately 10 mbsf, and the water content at depths below the seafloor was almost the same as that at SAKATA (Fig.5).

The normalized water content at SAKATA decreased with depth from approximately 1.1 near the seafloor surface to approximately $w/w_L = 0.7-0.8$ at depths below approximately 20 mbsf. The normalized water content is the value obtained by

dividing the natural water content w by the liquid limit w_L [15]. If the initial state of formation of the seafloor is when the bottom mud settles in almost one place and begins to consolidate under its own weight, Tsuchida estimated the water content at that time to be approximately $1.5 w_L - 2.0 w_L$, indicating that the normalized water content decreases with increasing depth [15]. The change in normalized water content with depth off the Sakata seafloor area was found to be similar to the results shown by Tsuchida.

Since the void ratio was obtained from the water content and soil particle density, the trend in the void ratio is almost the same as that of the water content. In both SAKATA and JOETSU, the void ratio decreased with increasing depth, reaching approximately $e=2.5$ at approximately 10 mbsf and approximately $e=2.0$ at depths greater than 20 mbsf. Tsuchida examined the process of strength development due to subsidence and sedimentation of the seafloor and subsequent consolidation under its own weight and showed the relationship between depth and void ratio for each sedimentation rate. The figure shows SCC ($1.5 e_L$) from the reference [19]. The SCC (Sedimentary Compression Curve) is a line that approaches the USC (Ultimate Standard Curve) as the consolidation pressure increases from being kneaded at a certain initial void ratio. Note that $1.5 e_L$ means that the initial void ratio is calculated as 1.5 times w_L . Comparing SCC($1.5 e_L$) with SAKATA, the void ratio change from the seafloor surface to approximately 35 mbsf is well represented. Since the void ratio tends to be larger in JOETSU than in the SCC ($1.5 e_L$), the initial void ratio at the time of deposition is considered to have been more than 1.5 times larger than that of w_L .

The void ratio of the offshore Sakata seafloor area decreases with depth from approximately 1.5 w_L near the seafloor surface to approximately $e=2.0$ at depths below approximately 20 mbsf, indicating that the change in the void ratio with depth is small. The void ratio of the off-Joetsu seafloor area tends to be larger than that of the off Sakata seafloor area at depths below approximately 20 mbsf, but the void ratio at depths below approximately 20 mbsf is almost the same as that of the off Sakata seafloor.

6. CONSOLIDATION PROPERTIES AND STRUCTURAL COEFFICIENTS

6.1 Results of The Incremental Loading Consolidation Test

From the results of the consolidation test using incremental loading, the relationship $\ln v - \log p$ is shown in Fig.10. The relationship between the coefficient of consolidation, coefficient of volume compressibility, and average consolidation pressure

is shown in Fig.11. The relationship between the average consolidation pressure divided by the consolidation yield stress and c_v is shown in Fig.12.

The relationship between C_c , p_c , and p_c divided by the effective soil overburden pressure, OCR and structural coefficient A is shown in Table 4. The relationship between depth and p_c , OCR, C_c , and structural coefficient A is shown in Fig.13. Here, structural coefficient A was proposed by Udaka et al. in a method to quantitatively evaluate the structure of natural clay using the compaction curve of naturally deposited clay obtained from consolidation tests [16]. Structural coefficient A is the difference between the specific volume and USC at p_c in the consolidation stress-volume ratio relationship.

If m_v is constant in the range $p > p_c$, then $\log m_v$ and $\log p$ show a linear relationship in that range. From Fig.11, it can be seen that except for Core 22, in which p_c is large, the relationship is as described above. c_v tends to be constant in the range of $p > p_c$. It has also been reported that c_v for cohesive and highly organic soils decreases rapidly around p_c with increasing consolidation stress [23]. Fig.12 shows the relationship between the average consolidation pressure divided by the consolidation yield stress and c_v . The figure shows c_v decreases from approximately 1×10^{-6} to approximately 1×10^{-7} before and after $p/p_c=1$, which is similar to the reference. However, the change is smaller for the shallow depth core. The relationship between c_v and p/p_c is almost the same regardless of depth, although the values tend to be larger for Core 22.

Table 4 and Fig.13 show that p_c increases linearly with increasing depth in both cores. C_c tends to be larger for older depositional ages and smaller with near unconfined ages [24]. With the exception of Core 37, both cores have $C_c =$ approximately 1 or less. Although greater depths are considered to indicate older depositional ages, C_c does not show an increasing trend, so there is no age effect on C_c .

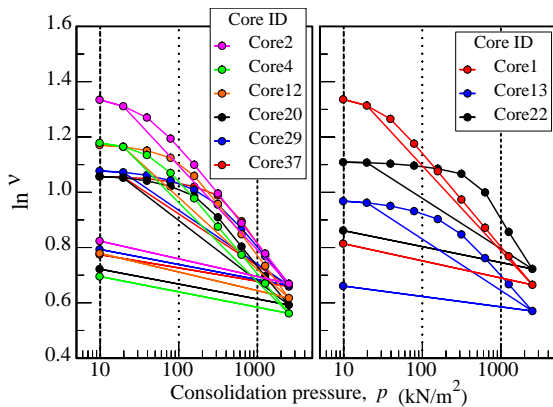


Fig.10 $\ln v - \log p$ relationship of Sakata Knoll

Table 4 Compression index, consolidation yield stress, OCR, Structural coefficient A

(a) RC2101A

Core ID	depth (mbsf)	C_c	p_c (kN/m ²)	OCR	structural coefficient A
Core 2	1.02 - 2.00	0.992	31.2	4.12	-0.076
Core 4	2.96 - 3.83	0.857	44.0	2.58	-0.049
Core 12	10.41 - 11.37	0.926	96.4	1.76	-0.045
Core 20	18.12 - 19.04	0.830	167.9	1.80	-0.023
Core 29	26.75 - 27.70	0.759	199.5	1.46	-0.051
Core 37	34.17 - 34.59	0.920	328.0	1.90	-0.015

(b) RC2102A

Core ID	depth (mbsf)	C_c	p_c (kN/m ²)	OCR	structural coefficient A
Core 1	0.00 - 0.98	1.023	26.9	10.94	-0.049
Core 13	25.37 - 25.88	0.639	191.3	1.49	-0.039
Core 22	54.30 - 55.12	1.203	467.6	1.70	-0.020

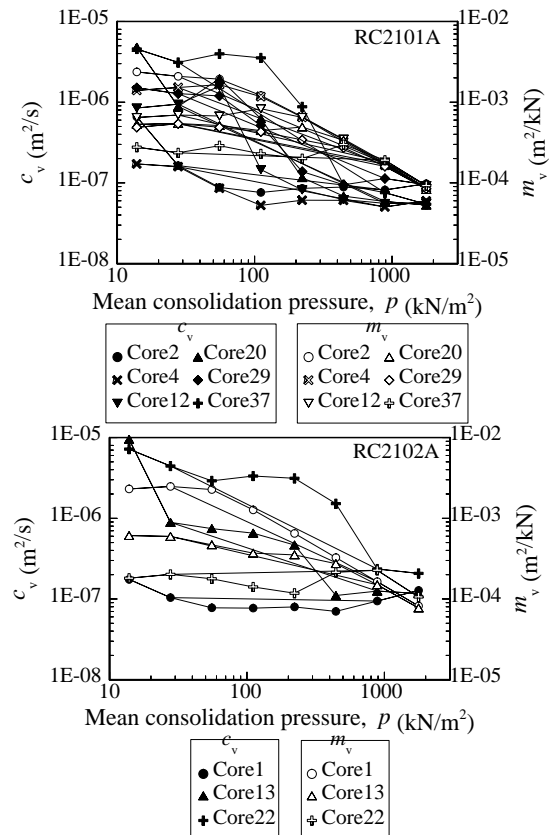


Fig.11 $\log c_v, \log m_v - \log p$ relationship of Sakata knoll

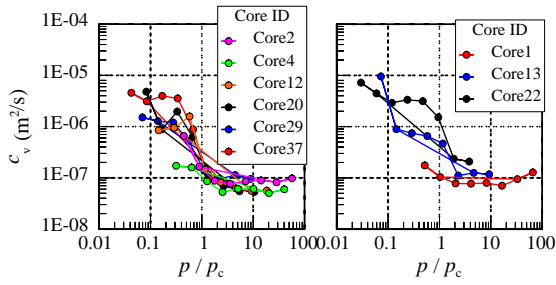


Fig.12 log c_v - log p/p_c relationship of Sakata Knoll

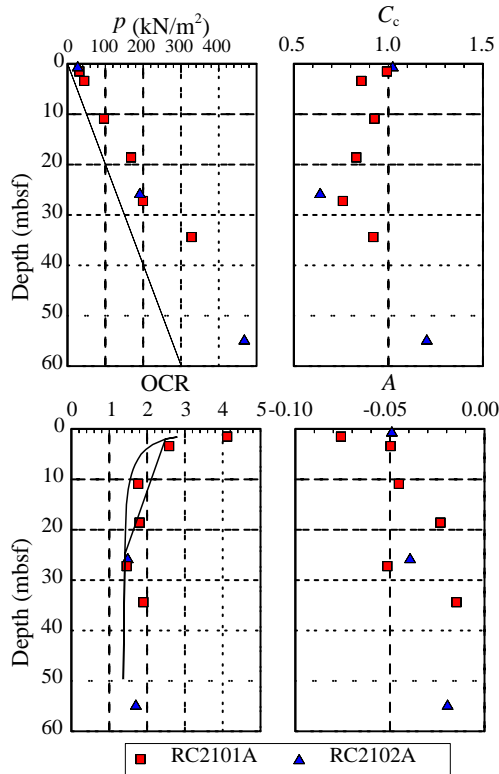


Fig. 13 Vertical distribution of measured consolidation properties and structural coefficient of clay in the Sakata Knoll

6.2 Consideration of OCR and structural coefficient A

The OCR decreased to approximately 12 mbsf in Core 12, and OCR=1.7 at depths below approximately 12 mbsf. This is similar to the trend observed in pseudo-overconsolidated clays, where the strength increases due to the age effect and overconsolidation occurs under constant overburden pressure after deposition without removal of overburden load. Tsuchida examined the process of strength development due to subsidence, sedimentation, and subsequent self-consolidation of the seafloor and determined the relationship between depth and OCR for each sedimentation rate. Since the sedimentation rate off the Sakata seafloor area is estimated to be 25-50 cm/ky [11], Fig.13

shows 0.01 cm/year from a literature reference [19]. Thus, a good match with the estimated value was found.

Udaka et al. [16] studied structural coefficient A using Japanese and foreign clays and reported that structural coefficient A is either constant regardless of depth or increases with depth from the seafloor surface and then becomes constant beyond a certain depth. For example, the structural coefficient A of alluvial clay in Osaka Bay increases up to approximately 7 mbsf, and the coefficient A below approximately 7 mbsf is 0.065. The structural coefficient A in SAKATA increased with increasing depth, and there was no tendency for the structural coefficient A to remain constant. The relationship between depth and structural coefficient A for RC2101A and RC2102A was different, and the increase in RC2101A seemed to be larger than that in RC2102A.

Udaka et al. show the relationship between depositional age and tectonic coefficient A for the Senshu alluvial and Pleistocene clays of Osaka Bay [16]. Based on the aforementioned depositional rates, the depositional age of the Sakata Knoll is estimated to be 60,000 to 120,000 years for approximately 30 mbsf and 110,000 to 220,000 years for approximately 55 mbsf.

Based on the relationship between depositional age and structural coefficient A shown by Udaka et al., the structural coefficient A for depositional ages of approximately 100,000 to 300,000 years is approximately 0.1 to 0.13. The maximum A of RC2101A and RC2102A is approximately A = -0.02. The A of RC2101A and RC2102A is approximately A = -0.02. The structural coefficient A in the Sakata Knoll is considerably smaller than that of the Osaka Bay alluvial clay, considering the depositional age of the clay, and in the MH formation area, the formation of carbonate nodules and changes in ion concentrations in pore water have been observed due to upwelling of methane in the subsoil [25-27]. This phenomenon is thought to affect mechanical properties, such as increased cohesion between soil particles due to the precipitation of carbonate minerals [28-33]. Structural factor A may also be affected, but RC2101A is not an MH-bearing area. Considering the depth variation in C_c , the degree of structural development of the Sakata Knoll is considered to be smaller than that of the Osaka Bay alluvial clay, irrespective of whether it is an MH-bearing area.

The structural coefficients of RC2101A and RC2102A are almost the same, indicating that the degree of structural development is less than that of Osaka Bay alluvial clay. Therefore, it can be said that the influence of MH presence on structural development is small. However, the strength of the methane flow is important for the formation of

carbonate nodules. The degree of structural development may differ at sites with different methane flux strengths, which is a topic for future study.

7. CONCLUSION

The results of the study are summarized below.

- 1) The soil particle density, grain size distribution, liquid limit, plastic limit, and plasticity index of RC2101A and RC2102A are almost the same regardless of depth up to approximately 55 mbsf.
- 2) The void ratios of RC2101A and RC2102A decreased with increasing depth, reaching approximately $e=2.5$ at approximately 10 mbsf and approximately $e=2.0$ at depths greater than 20 mbsf. This trend is similar to that observed in the Umitaka Spur and Joetsu Basin.
- 3) The structural coefficient A increased with increasing depth, confirming that structure develops with increasing depth in both RC2101A and RC2102A.
- 4) A comparison of the relationship between the depositional age and the structural coefficient A, which was generated from the Osaka Bay Pleistocene clay and Osaka Bay Alluvial clay, and the change in C_c in the depth direction indicates that the degree of structural development is small for both RC2101A and RC2102A.
- 5) The effect of MH availability on clay structure development is considered to be small.

8. ACKNOWLEDGMENTS

This study was conducted as a part of the methane hydrate research project funded by METI (the Ministry of Economy, Trade and Industry, Japan). We would like to express our gratitude to Professor Takao Ebinuma of the Faculty of Engineering, Tottori University, for various suggestions in the course of our research. We would like to thank everyone involved.

9. REFERENCES

- [1] Sloan E. D., Jr., Clathrate Hydrates in Natural Gases, 2nd edition, Marcel Dekker Inc, 1998, pp. 33-34.
- [2] Monozawa N., Kaneko M. and Ozawa M., A review of petroleum system in the deep water area of the Toyama Trough to the Sado Island in the Japan Sea, based on the results of the METI Sado Nansei Oki Drilling, Journal of the Japanese association for Petroleum technology, Vol.71, No.6, 2006, pp. 618-627.
- [3] Matsumoto R., Okuda Y., Hiruta A., Tomaru H., Takeuchi E., Sanno R., Suzuki M., Tsuchinaga K., Ishida Y., Ishizaki O., Takeuchi R., Komatsubara J., Fernando FREIRE A., Machiyama H., Aoyama C., Joshima M., Hiromatsu M., SNYDER G., Numanami H., Satoh M., Matoba Y., Nakagawa H., Kakuwa Y., Ogihara S., Yanagawa K., Sunamura M., Goto T., Lu H. and Kobayashi T., Formation and Collapse of Gas Hydrate Deposits in High Methane Flux Area of the Joetsu Basin, Eastern Margin of Japan Sea, Vol.118, No.1, 2009, pp. 43-71.
- [4] Matsumoto R., Kakuwa Y., Tanahashi M. and MD179 Shipboard Scientists, Occurrence and origin of shallow gas hydrates of the eastern margin of Japan Sea as revealed by CALYPSO and CASQ corings of R/V Marion Dufresne. Proceedings of the 7th International Conference on Gas Hydrates (ICGH 2011), 2011, pp.17-21.
- [5] Matsumoto R., Takahashi M., Kakuwa Y., Snyder G., Ohkawa S., Tomaru H., and Morita S., Recovery of thick deposits of massive gas hydrates from gas chimney structures, eastern margin of Japan Sea Japan Sea shallow gas hydrate project, National energy technology laboratory, Fire in the ice, Vol.17, Issue 1, Methane hydrate news letter, 2017, pp. 1-6.
- [6] Ministry of Economy, Trade and Industry, Research and development of surface-type methane hydrate, The 38th Methane hydrate development and implementation review Meeting, https://www.meti.go.jp/shingikai/energy_environment/methane_hydrate/pdf/038_05_00.pdf, 2021.
- [7] Yamamoto K., Boswell R., Collett T S., Dallimore S R, and Lu, H., Review of Past Gas Production Attempts from Subsurface Gas Hydrate Deposits and Necessity of Long-Term Production Testing, Energy Fuels, Vol.36, No.10, 2022, pp.5047-5062.
- [8] Yoneda J., Masui A., Konno Y., Jin Y., Egawa K., Kida M., Ito T., Nagao J., and Tenma N., Mechanical behavior of hydrate-bearing pressure-core sediments visualized under triaxial compression, Marine and Petroleum Geology, Vol.66, 2015, pp. 451-459.
- [9] Yoneda J., Masui A., Konno Y., Jin Y., Egawa K., Kida M., Ito T., Nagao J., and Tenma N., Mechanical properties of hydrate-bearing turbidite reservoir in the first gas production test site of the Eastern Nankai Trough, Marine and Petroleum Geology, Vol.66, 2015, pp. 471-486.
- [10] Yamamoto K. and Tenma N., Development of Methane Hydrate Resources - Issues for Commercialization and Their Current R & D Status, Marine Engineering, Vol.56, 2021, pp.244-250.
- [11] Katayama H. and Itaki T., Spatial distribution of sedimentation rates in the eastern Japan Sea off Akita, Jour. Geol. Soc. Japan, Vol.113, No.10, 2007, pp.505-518.
- [12] Oi T., Akiba F., and Matsumoto R., Characteristics of sedimentation rates around hydrate seep area in the eastern part of Japan Sea, Japan Geoscience Union MEETING2016, 2016, MIS09-P04.
- [13] Jamiolkowski M., Ladd C. C., Germaine J. T., and

- Lancellota R., New developments in field and laboratory testing of soils, 11th International Conference on Soil Mechanics and Foundation Engineering, 1985, pp.57-153.
- [14] Burland J. B., On the compressibility and shear strength of natural clays, *Géotechnique*, Vol.40, No. 3, 1990, pp.329-378.
- [15] Tsuchida T., General Interpretation on Natural Void Ratio-Overburden Pressure Relationship of Marine Deposits, *Journal of the Japanese Geotechnical Society*, Vol.41, No.1, 2001, pp.127-143.
- [16] Udaka K., Tsuchida T., Watabe Y., Tanaka M. and Imai Y., Study on estimation of structures of natural marine clay deposits using a simple model of $e - \log p$ curves Study on estimation of structures of natural marine curves, *Japanese Geotechnical Journal*, Vol.7, No.4, 2012, pp.527-542.
- [17] Oono K. and Nakamura K., Physical properties of clay from the Joetsu Basin in the eastern margin of the Japan Sea, 57th Japan National Conference on Geotechnical Engineering, 2021, 13-4-2-04.
- [18] Goto S., Yamano M., Morita S., Kanamatsu T., Hachikubo A., Kataoka S., Tanahashi M., and Matsumoto R., Physical and thermal properties of mud-dominant sediment from the Joetsu Basin in the eastern margin of the Japan Sea, *Marine Geophysical Research*, Vol.38, No.44, 2017, pp.393-407.
- [19] Tsuchida T., Structure due to cementation of Osaka bay clay and its mathematical modeling, *Proceedings of the Symposium on Geotechnical Aspects of Kansai International Airport*, 2005, pp.31-40.
- [20] Okamura Y., Relationships between geological structure and earthquake source faults along the eastern margin of the Japan Sea, *Jour. Geol. Soc. Japan*, Vol.116, No.11, 2010, pp.582-591.
- [21] Asada M., Satoh M., Tanahashi M., Yokota T. and Goto S., Visualization of shallow seafloor fluid migration in a shallow gas hydrate field using high-resolution acoustic mapping and ground-truthing and their implications on the formation process: a case study of the Sakata Knoll on the eastern margin of the Sea of Japan: *Marine Geophysical Research*, Vol.43, 2022, Article number 34.
- [22] A.W. Skempton, Activity of clays, *Proc. 3rd Int. Conf. on SMFE*, 1953, pp.195-200.
- [23] Tavenas F., Leblond P., Le Bihan J. -P. and Leroueil S., The permeability of natural soft clays, *Canadian Geotechnical Journal*, Vol.20, No.4, 1983, pp.629-660.
- [24] Kansai Branch of The Japanese Geotechnical Society, *Submarine Subsoil: Osaka Bay as an Example*, 1995, pp.146-168.
- [25] Aizawa S., and Matsumoto R., Mineralogical and chemical compositions of carbonate nodules collected by MD-179 research cruise, *Journal of the Japanese Association for petroleum Technology*, Vol.77, No.6, 2012, pp.460-465.
- [26] Kamei T., Tokuoka T., Sampei Y., and Ishihara H., *Geotechnology and Sedimentary Environment of Holocene Deposits in the Matsue plains*, *Jour. Japan Soc. Eng. Geol.*, Vol.38, No.5, 1997, pp.280-295.
- [27] Minami H., Sakagami H., Hachikubo A., Yamashita S., Shoji H. and Takahashi N., Sub-bottom methane hydrates off northeastern Sakhalin Island, Russia -Evaluation of methane flux by dissolved ions in the sediment pore waters-, *Low Temperature Science*, Vol.74, 2016, pp.153-161.
- [28] Kataoka S., Yamashita S., Minami H., Nishio S., Abe T., Yokoyama T., Hyodo M. and Grachev M., Geotechnical properties of the shallow type methane hydrate-bearing sediments in the Lake Baikal, *Japanese Geotechnical Journal*, Vol.2, No.2, 2007, pp.95-105.
- [29] Yamashita S., Dewa H., Hachikubo A., Minami H., Kataoka S., Kawaguchi T., Sakagami H., Takahashi N. and Shoji H., Soil properties of sediments obtained from sea and lake-bottom shallow type gas hydrate province - Evaluation of sample disturbance due to exsolution of dissolved gas in pore water -, *Japanese Geotechnical Journal*, Vol.7, No.4, 2012, pp. 503-516.
- [30] Kataoka S. and Matsumoto R., The physical and mechanical properties of sea-bottom sediments in the eastern margin of Japan Sea by MD179, *Vol.77, No.4, 2012, pp. 274-279.*
- [31] Miura R., Yamashita S., Minami H., Hachikubo A., Sakagami H., Takahashi N., Shoji H., Matsumoto R., Jin Y. K., Obzhirov A. and Khlysov O., Soil properties of deep lake and sea bottomsediments, *Geotechnical Engineering Society of Japan Hokkaido Branch Technical Report Collection*, Vol.53, 2013, pp. 49-58.
- [32] Yoneda J., Kida M., Konno Y., Jin Y., Morita S., Tenma N., In situ mechanical properties of shallow gas hydrate deposits in the deep seabed, *Geophysical Research Letters*, No.46, 2019, pp. 14459-14468.
- [33] Aoki S., Kyono S., Oi T., Owari S., Akiba F., Ochiai H., Tomaru H., Noborio K. and Matsumoto R., Soil properties of subsurface sediments collected from shallow gas hydrate province in the eastern margin of the Japan Sea, *Journal of the Sedimentological Society of Japan* Vol. 76, No. 2, 2018, pp. 61-75.